



Journal of Advanced Research in Applied Mechanics

Journal homepage:
https://semarakilmu.com.my/journals/index.php/appl_mech/index
ISSN: 2289-7895



Dynamic Modelling of the Spine for the Estimation of Vertebral Joint Torques using Gordon's Method

Munawwarah Solihah Muhammad Isa¹, Nurhidayah Omar^{1,2,*}, Mohammad Shahril Salim², Saidatul Ardeenawatie Awang², Suhizaz Sudin²

¹ Institute of Engineering Mathematics, Universiti Malaysia Perlis (UniMAP), 02600 Arau, Perlis, Malaysia

² Sport Engineering Research Centre, Faculty of Electronic Engineering & Technology, Universiti Malaysia Perlis, 02600 Arau, Perlis, Malaysia

ARTICLE INFO

Article history:

Received 22 July 2024

Received in revised form 24 August 2024

Accepted 1 September 2024

Available online 30 September 2024

ABSTRACT

World Health Organization (WHO) recognised musculoskeletal disorder (MSD) as the main contributor to disability worldwide, with low back pain as the major disorder globally. The occupational disorder normally occurs during lifting. The weight of the load and manual handling tasks during lifting has an impact on the spine and joint torque. The purpose of this study is to propose a dynamic model of the spine that can estimate the vertebral joint torques. This study is a bimodal approach that consists of the experimental and theoretical parts. Ten healthy UniMAP students (10 males) participated in this study. The subjects were required to lift a 3kg weight plate for kinematics and EMG data collection. Retro-reflective markers were attached to the subject body, and then, the data was collected and stored in QTM software. Kinematic data was processed using C-Motion Visual3D. Eight Trigno Wireless Sensors were attached on the back muscles (left and right erector spinae, latissimus dorsi, external oblique and internal oblique). The EMG data were stored in EMG Acquisition software and subsequently, were processed using EMG Analysis software. Gordon's method was used to develop a mathematical model of the spine. The model comprises of five kinematic chains which connected three lumbar, two thoracic and one cervical. The model calculated the value of joint torque on flexion/extension movement using Matlab and Microsoft Excel. When calculated on L5, the model gives an estimation within 0 – 30 kgm²s⁻². The model was further used to estimate value of L3, L1, MAI and T2. The estimate average value of joint torque at L3 is within 5 – 25 kgm²s⁻², MAI is within 0 – 6 kgm²s⁻² and T2 is within 0 – 1 kgm²s⁻². The average RMS values show the highest muscle activity on the right internal oblique muscle (1519 µV), followed by the right external oblique (1166 µV) and left external oblique (418 µV). The results obtained gives an insight on the value of joint torque that have been applied by the spine and the most activated back muscles during lifting.

Keywords:

Musculoskeletal Disorder (MSD); Lifting; Spine; Mathematical model

1. Introduction

MSD is the injury or pain that can affect the muscles, bones, and joints. This disease may be correlated to work, daily life or age, and affect musculoskeletal system. Tendonitis, epicondylitis,

* Corresponding author.

E-mail address: hidayahomar@unimap.edu.my

<https://doi.org/10.37934/aram.125.1.4257>

osteoarthritis, muscle strain, back pain and trigger finger are some of the MSDs that can develop with continuous overworking. Too much force and repetition, poor posture, poor work practices, poor fitness and poor health habits are the risk factors that lead to MSD [1]. Unsuitable body position or awkward posture made the joint weaker or likely to become injured. Awkward postures can lead to fatigue and increase the chance to develop MSD. In the workplace, fatigue happens when the employees exposed to MSD risk factors. MSD became one of the reasons of why the labour forces in occupational population are declining [2]. As fatigue overtakes body's recovery system, musculoskeletal imbalance is developed. Likewise, MSD can affect any part of the body such as low back, neck, shoulder and hand. Low back MSD include spinal disc problems, muscle and tissue injuries. These disorders correlated with physical work such as pushing, pulling, bending, twisting and lifting heavy loads. Activities that require lot of strength will affect the muscle, torso, joints and spinal disc. Working with correct posture can reduce stress on the back and on the extremities, while an unsuitable posture will increase spinal stress [3].

Numerous researchers have tried to develop methods which include experimental and analytical approach. Various models have been utilised to analyse the spinal loads. In the past decades, Panjabi *et al.*, [4] constructed three-dimensional mathematical models and developed equations of motion based on spine structure. Three years later, Panjabi *et al.*, [5] used mathematical model to predict the biomechanical behaviour of the spine where the focused of the study was at thoracic part. The study used values from experiment and then correlated the model behaviour to predict real spine behaviour. Meanwhile, a study by Bassani *et al.*, [6] used model to analyse lumbar spine loads at L4-L5 level. Actis *et al.*, [7] also examined a musculoskeletal model with a detailed lumbar spine to predict the loads on L4-L5. Another study by Harari *et al.*, [8] analysed the biomechanical loads and kinematics during material handling tasks and developed models for the moments acting on a worker's body. Selamat *et al.*, [9] develop a hybrid exoskeleton to study movement during oil palm harvesting work. The movement includes lifting up, holding pole up and walk, elbow extension-flexion and lifting up-down the pole.

Previous studies on mathematical model of the spine develops the model of the spine by separating the spine into different parts, either on the cervical, thoracic or lumbar vertebrae. The intention of this study is to develop a three-dimensional dynamic model of the spine that includes joints on cervical, thoracic and lumbar vertebrae. The three-dimensional model of lifting behaviour is developed using Gordon's method. Gordon used Kane's method to formulate the dynamic equations of motion for a planar linkage having an arbitrary number of links which allowed the n dynamic equations for an n-link planar linkage to be written down without having to derive them [10]. Kane's method is a vector-based approach which used vector cross and dot products to obtain velocities and accelerations. Gordon's method is constrained to open, unbranched kinematic chains and requires segmental angles as the generalized coordinates. Gordon's method benefit is that the dynamic equations are written in their most compact form, which is where the mass Matrix M is symmetric, positive semi-definite. This method also easy and less time consuming, so the result can be produced in short time compared to Kane's method as the equations are derived accurately [11]. Lifting includes movements such as standing – bending forward – lifting a weight – standing. These movements when being done repetitively might put a risk to develop musculoskeletal disorder [9]. In this study, the subject will perform lifting movements. The mathematical model will be used to estimate the value of joint torques on cervical, thoracic and lumbar vertebrae. The results will give some insight on the joint that produce highest value of joint torque during lifting movement.

2. Methodology

2.1 Data Collection

2.1.1 Subjects

The subjects participated in this study are limited to a total of 7 male students at University Malaysia Perlis (UniMAP) where the research was carried out in the biomechanics laboratory at Faculty of Mechanical Engineering in UniMAP. Before subject participates in the study, each subject will be briefed the purpose of study. All subjects were provided with the informed consent to the research protocol. Table 1 shows the detail of subjects used in this study:

Table 1
Anthropometric characteristic of study cohort

Variable	Mean \pm SD
Age (years)	24
Body height (m)	1.73 \pm 0.05
Body mass (kg)	72.5 \pm 14.78

2.1.2 Kinematic data collection

The kinematic data was collected in Biomechanics lab using Qualisys Track Manager System. Before the recording, subject was explained regarding the data collection procedures, and an informed consent form was signed. The procedure is in accordance with the Universiti Malaysia Perlis ethical guidelines. The subject was required to perform standing-bending-lifting movement as in Figure 1. The total of 10 trials for each subject was recorded by infrared reflective cameras sampling at a frequency of 100 Hz.

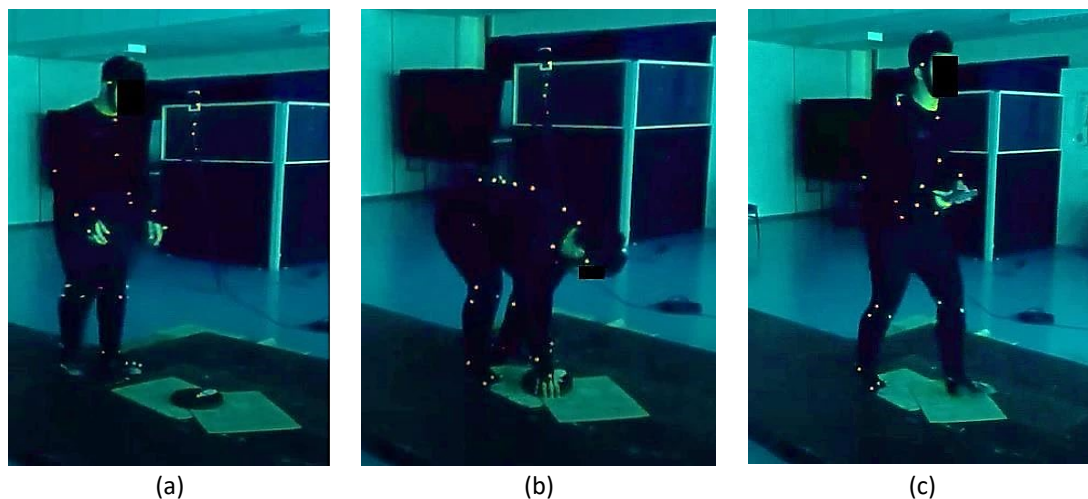


Fig. 1. A subject performing (a) standing (b) bending (c) lifting movement with reflective markers attached to the subject's body

To observe the spine activity during the standing-bending-lifting movement, eight markers were attached on the right and left posterior superior iliac spines (RPSIS and LPSIS), the midpoint between the inferior angles of most caudal points of the two scapulae (MAI), the seventh cervical vertebra (C7), the second thoracic vertebra (T2), and of the first, third, and fifth lumbar vertebra (L1, L3, and L5). The markers attachment is shown as in Figure 2. The selection of points for marker attachment on the spine is following the study by Leardini *et al.*, [12]. The five best standing-bending-lifting trials

with no marker loss were selected and processed using Visual 3D software to calculate the segmental motion data.

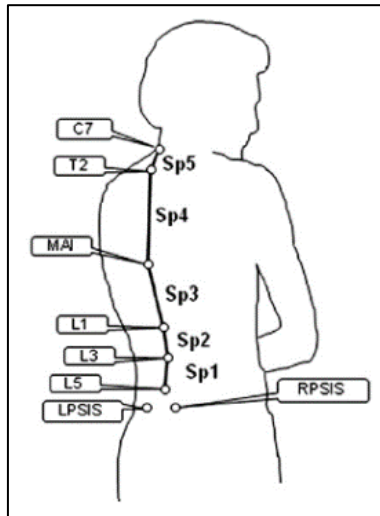


Fig. 2. The location of markers attached on the spine

2.1.3 EMG data collection

Eight Trigno Avanti Wireless Sensors were placed on subject skin at the back muscles on different locations (Figure 3). Four back muscles were chosen for this experiment: left and right erector spinae, left and right latissimus dorsi, left and right external obliques and left and right internal obliques following the previous studies [13-15].

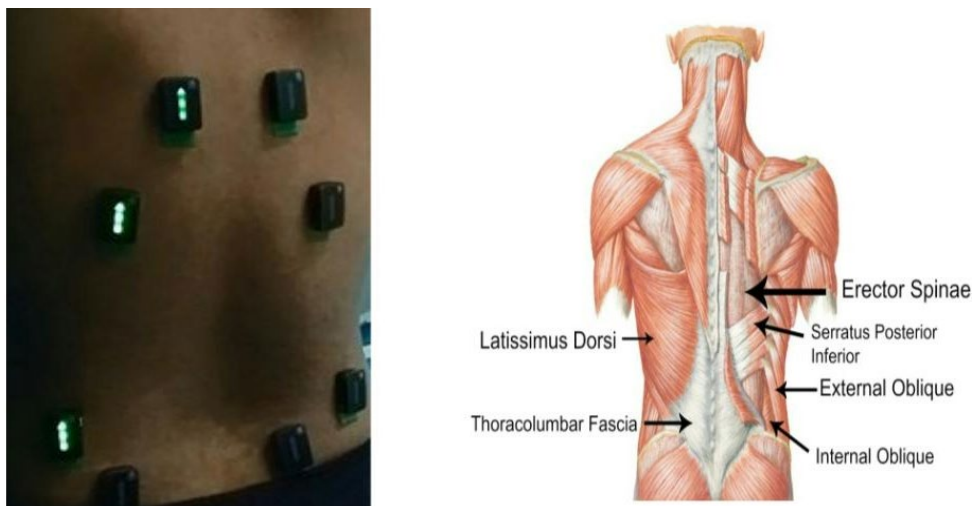


Fig. 3. The location of Trigno Avanti Wireless Sensors on back muscles

Sensor configuration and collection of data were initiated using Trigno software called EMG works Acquisition installed on a PC. The base station is connected to the PC via the USB port to acquire data. However, it is important to ensure that the sensors are paired to the base station to provide wireless conveyance to the base station and to transmit the collected data to the EMG works Acquisition from the base station. This pairing can be done by placing the sensors on the base station magnet where

the sensors will blink green to indicate a successful pair and only after that the sensors can be put on the skin. This study used Delsys EMGs (Trigno™ Wireless System, Delsys Incorporated, Natick, USA) with acquisition frequency of 1000 Hz as in previous studies [16-19].

2.1.4 Lifting data collection procedure

Details of the experiment protocol were explained to the subjects. The weight and height of the subjects were measured and recorded. Each of body segments was measured. The 28 markers were placed on the subject's body. Before the subjects start to lift the weight plate, they need to stand on the platform for QTM to capture the static posture through the cameras. The static trial was necessary so that the model could be appropriately scaled and applied to the subject. Based on Manual Handling Guideline & Regulations from DOSH, recommended lifting weight for men is 10kg at the limit and for women it is at 7 kg at the limit. Following the guidelines, the load used in this experiment is only 3kg (minimum weight for men and women) to avoid unnecessary consequences to the subject such as back pain. To start the experiment procedure, a weight plate of 3 kg was placed on the platform and the subject need to lift it. All the six cameras captured the movement of the subject. Subjects performed 10 trials where each trial is recorded separately. Kinematic data and EMG data collection were recorded and collected simultaneously.

2.2 Data Processing

2.2.1 Kinematic data processing

Each flexion-extension angle from orientation of the trunk segment for each subject was calculated in Visual3D using an X-Y-Z (flexion/extension, medial/lateral rotation and abduction/adduction) Cardan rotation sequence. Visual3D used marker trajectories to model and to define segment properties such as the segments proximal and distal ends, and the segments geometry. To do this, the imported dynamic files were assigned to static files. Static file contains all the markers used during experiment so that all the segments can be defined. All tracked and labelled trials in QTM were exported and save as .c3d file into Visual3D™ (Version 3.91, C-Motion, USA) and run through the Visual3D for the model building and to process the needed kinematics data. Before building the model, the markers were interpolated and filtered. Following the Visual3D tutorial of signal processing, a 3rd order polynomial was used to interpolate the marker trajectories and was filtered using low-pass Butterworth filter with a 6.0 Hz cut-off frequency [20]. To build the model, the static trial .c3d file loaded to Visual3D.

The purpose of the anatomy model building is to analyse the movement of the skeletal system under the markers. In this study, pelvis acted as the base segment of the model, followed by the thorax, left and right upper arm, left and right forearm, left and right hand and lastly, left and right thigh. The model uses global optimisation to determine the position of the segments and their direction of orientation. Each segment has its own coordinate system, which is at a specific transformation relative to the global or laboratory coordinates system.

2.2.2 EMG data processing

The collected muscles data were saved as .hpf file in the PC. Data collected using Delsys EMG wireless sensors were processed using the EMG works Analysis software as suggested in previous studies [21,22]. EMG works Analysis was used to process all the EMG signals and the results are exported into Excel as .txt file.

2.3 Data Analysis

The orientation of flexion-extension for the spinal vertebrae was determined using calculations in Visual3D. The obtained angles for each part were exported to MATLAB. Mathematical data was developed using Matlab (version R2019a 9.6.0.1072779, MathWorks, Natick, MA, USA). Data was exported from Excel .txt file and computed in MATLAB using the mathematical model.

Next, using the Root Mean Square (RMS) function, the square root of the energy contained in the EMG signal was calculated for each sensor to provide a parameter for studying muscle strength during lifting activity [20]. According to Nur *et al.*, [23], the RMS value correlate with the square root of the average power of the raw EMG signal in a given period of time. The RMS used to determine the muscle signals is expressed as follows:

$$RMS = \sqrt{\frac{1}{N} \sum_{i=1}^N x_i^2} \quad (1)$$

2.4 Mathematical Model

Figure 4 illustrates the position of spinal vertebrae when lifting. There are five kinematic chains involved in this which are segment A, B, C, D and E. N is the pelvis which is the reference frame for this model where the segmental angles are measured by referring to it. Segment A includes the part of N to L5, segment B from L5 to L3, segment C from L3 to L1, segment D from L1 to T7 and segment E from T7 to T2. ρ is the length of segment which includes part from end of proximal to mass center, l is the total length of segment.

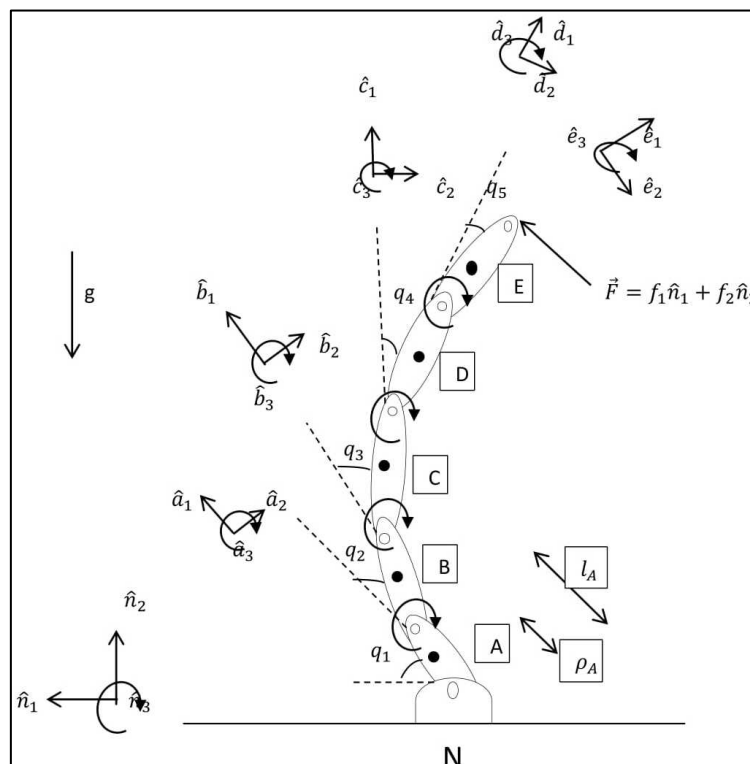


Fig. 4. Five kinematic chains represent the spinal vertebrae during lifting activity

Rigid bodies of A, B, C, D, E and the reference frame N are joined together with frictionless pins at the endpoint of each segment (circle with no fill). These endpoints were referred as A_0 , B_0 , C_0 , D_0 and E_0 . Triads of mutually perpendicular unit vectors define vector component directions for each of these four rigid body reference frames. The mass centroids (circle with fill) referred as A^* , B^* , C^* , D^* and E^* for the respective bodies are located at distances ρ_A , ρ_B , ρ_C , ρ_D and ρ_E from their proximal ends. A torque $\tau_{N/A}$ is exerted by N on A, torque $\tau_{A/B}$ is exerted by A on B, torque $\tau_{B/C}$ is exerted by B on C, torque $\tau_{C/D}$ is exerted by C on D, torque $\tau_{D/E}$ is exerted by D on E. An endpoint force of arbitrary direction and magnitude, $\vec{F} = f_1 \hat{n}_1 + f_2 \hat{n}_2$ is exerted by an external influence at the endpoint of the linkage, D_0 .

2.5 Anthropometric Data

To ensure an accurate measurement, the total length of the segment was obtained from a study conducted by Singh *et al.*, [24]. The subject used in previous study is in agreement with the average height and weight of the subjects in this study where only male subjects were included. Based on the model, the total length of the segment is represented by l_A , l_B , l_C , l_D , l_E and l_F . The distance between the proximal and the centre of each segment mass is represented by notation ρ_A , ρ_B , ρ_C , ρ_D , ρ_E and ρ_F . The segment masses were needed for calculating gravitational forces and linear inertial terms, and to estimate the segment moments of inertia from angular inertial terms. The mass of each segment is represented by the notations m_A , m_B , m_C , m_D , m_E and m_F as found in the model. The mass of each segment is calculated based on the mass of the subjects and the mass fraction of each segment. The mass of each vertebral body mass was based on the predictions by Pearsall *et al.*, [25]. This study was corresponded to the average mass and height of subjects' body and they varied by less than one percent. The moment of inertia of the center of mass of each segment is represented by the notation I_A , I_B , I_C , I_D , I_E and I_F as found in the model. Table 2 shows the estimate mass, inertia and length for vertebral segments.

Table 2
 Mass, inertia and length estimates of vertebral segments

Segment	Mass (kg)	Inertia (kgm ²)	Length (m)
Segment 1 (L5-L3)	5.2926	0.00963	0.07629
Segment 2 (L3-L1)	5.0356	0.00926	0.07671
Segment 3 (L1-MAI)	9.4636	0.06754	0.151125
Segment 4 (MAI-T2)	5.5277	0.01977	0.10698
Segment 5 (T2-C7)	2.4054	0.00156	0.04549

2.6 Gordon's Method

The generalised coordinates for a five planar linkage are defined using segmental angles measured from a horizontal plane. The following equation is the auxiliary variables; μ , δ and γ for the spine:

Auxiliary variables:

$$\mu_1 = l_A(m_B + m_C + m_D + m_E) \quad (2)$$

$$\mu_2 = l_B(m_C + m_D + m_E) \quad (3)$$

$$\mu_3 = l_C(m_D + m_E) \quad (4)$$

$$\mu_4 = l_D(m_E) \quad (5)$$

$$\mu_5 = 0 \quad (6)$$

$$\delta_1 = \frac{l_A^2(m_B+m_C+m_D+m_E)+I_A+m_A\rho_A^2}{l_A} \quad (7)$$

$$\delta_2 = \frac{l_B^2(m_C+m_D+m_E)+I_B+m_B\rho_B^2}{l_B} \quad (8)$$

$$\delta_3 = \frac{l_C^2(m_D+m_E)+I_C+m_C\rho_C^2}{l_C} \quad (9)$$

$$\delta_4 = \frac{l_D^2(m_E)+I_D+m_D\rho_D^2}{l_D} \quad (10)$$

$$\delta_5 = \frac{I_E+m_E\rho_E^2}{l_E} \quad (11)$$

$$\gamma_1 = l_A m_B + l_A m_C + l_A m_D + l_A m_E + m_A \rho_A \quad (12)$$

$$\gamma_2 = l_B m_C + l_B m_D + l_B m_E + m_B \rho_B \quad (13)$$

$$\gamma_3 = l_C m_D + l_C m_E + m_C \rho_C \quad (14)$$

$$\gamma_4 = l_D m_E + m_D \rho_D \quad (15)$$

$$\gamma_5 = m_E \rho_E \quad (16)$$

Mass Matrix, M:

$$M_{11} = l_A^2 m_B + l_A^2 m_C + l_A^2 m_D + l_A^2 m_E + I_A + m_A \rho_A^2 \quad (17)$$

$$M_{22} = l_B^2 m_C + l_B^2 m_D + l_B^2 m_E + I_B + m_B \rho_B^2 \quad (18)$$

$$M_{33} = l_C^2 m_D + l_C^2 m_E + I_C + m_C \rho_C^2 \quad (19)$$

$$M_{44} = l_D^2 m_E + I_D + m_D \rho_D^2 \quad (20)$$

$$M_{55} = I_E + m_E \rho_E^2 \quad (21)$$

$$M_{12} = m_C l_A l_B \cos q_1 - m_C l_A l_B \cos q_2 + m_D l_B l_A \cos q_1 - m_D l_A l_B \cos q_2 + m_E l_A l_B \cos q_1 - m_E l_A l_B \cos q_2 + m_B l_A \rho_B \cos q_1 - m_B l_A \rho_B \cos q_2 \quad (22)$$

$$M_{13} = m_D l_A l_C \cos q_1 - m_D l_A l_C \cos q_3 + m_E l_A l_C \cos q_1 - m_E l_A l_C \cos q_3 + m_C l_A \rho_C \cos q_1 - m_C l_A \rho_C \cos q_3 \quad (23)$$

$$M_{14} = m_E l_A l_D \cos q_1 - m_E l_A l_D \cos q_4 + m_D l_A \rho_D \cos q_1 - m_D l_A \rho_D \cos q_4 \quad (24)$$

$$M_{15} = m_E l_A \rho_E \cos q_1 - m_E l_A \rho_E \cos q_5 \quad (25)$$

$$M_{23} = m_D l_B l_C \cos q_2 - m_D l_B l_C \cos q_3 + m_E l_B l_C \cos q_2 - m_E l_B l_C \cos q_3 + m_C l_B \rho_C \cos q_2 - m_C l_B \rho_C \cos q_3 \quad (26)$$

$$M_{24} = m_E l_B l_D \cos q_2 - m_E l_B l_D \cos q_4 + m_D l_B \rho_D \cos q_2 - m_D l_B \rho_D \cos q_4 \quad (27)$$

$$M_{25} = m_E l_B \rho_E \cos q_2 - m_E l_B \rho_E \cos q_5 \quad (28)$$

$$M_{34} = m_E l_C l_D \cos q_3 - m_E l_C l_D \cos q_4 + m_D l_C \rho_D \cos q_3 - m_D l_C \rho_D \cos q_4 \quad (29)$$

$$M_{35} = m_E l_C \rho_E \cos q_3 - m_E l_C \rho_E \cos q_5 \quad (30)$$

$$M_{45} = m_E l_D \rho_E \cos q_4 - m_E l_D \rho_E \cos q_5 \quad (31)$$

$$M_{21} = m_{12} \quad (32)$$

$$M_{31} = m_{13} \quad (33)$$

$$M_{32} = m_{23} \quad (34)$$

$$M_{41} = m_{14} \quad (35)$$

$$M_{51} = m_{15} \quad (36)$$

$$M_{42} = m_{24} \quad (37)$$

$$M_{43} = m_{34} \quad (38)$$

Vector of Applied Torques, \vec{T}

$$T_1 = (\tau_{N/A} - \tau_{A/B}) \cdot \hat{n}_3 \quad (39)$$

$$T_2 = (\tau_{A/B} - \tau_{B/C}) \cdot \hat{n}_3 \quad (40)$$

$$T_3 = (\tau_{B/C} - \tau_{C/D}) \cdot \hat{n}_3 \quad (41)$$

$$T_4 = (\tau_{C/D} - \tau_{D/E}) \cdot \hat{n}_3 \quad (42)$$

$$T_5 = (\tau_{D/E}) \cdot \hat{n}_3 \quad (43)$$

Vector of moments from gravitational forces, \vec{G}

$$G_1 = -m_B g(l_A \cos q_1) - m_C g(l_A \cos q_1) - m_D g(l_A \cos q_1) - m_E (l_A \cos q_1) - m_A g(\rho_A \cos q_1) \quad (44)$$

$$G_2 = -m_C g(l_B \cos q_2) - m_D g(l_B \cos q_2) - m_E g(l_B \cos q_2) - m_B g(\rho_B \cos q_2) \quad (45)$$

$$G_3 = -m_D g(l_C \cos q_3) - m_E g(l_C \cos q_3) - m_C g(\rho_C \cos q_3) \quad (46)$$

$$G_4 = -m_E g(l_D \cos q_4) - m_D g(\rho_D \cos q_4) \quad (47)$$

$$G_5 = -m_E g(\rho_E \cos q_5) \quad (48)$$

Vector of moments from external forces and torques, \vec{E}

$$E_1 = f_2(l_A \cos q_1) - f_1(l_A \sin q_1) \quad (49)$$

$$E_2 = f_2(l_B \cos q_2) - f_1(l_B \sin q_2) \quad (50)$$

$$E_3 = f_2(l_C \cos q_3) - f_1(l_C \sin q_3) \quad (51)$$

$$E_4 = f_2(l_D \cos q_4) - f_1(l_D \sin q_4) \quad (52)$$

$$E_5 = f_2(l_E \cos q_5) - f_1(l_E \cos q_5) \quad (53)$$

The equations of motion can be written in the matrix form:

$$M\ddot{Q} = \vec{T} + \vec{E} + \vec{G} \quad (54)$$

$$\begin{bmatrix} I_A^2 m_B + I_A^2 m_C + I_A^2 m_D + I_A^2 m_E + I_A + m_A \rho_A^2 & m_C l_A l_B \cos q_1 - m_C l_A l_B \cos q_2 + m_D l_B l_A \cos q_1 - m_D l_A l_B \cos q_2 + m_E l_A l_B \cos q_1 - m_E l_A l_B \cos q_2 + m_B l_A \rho_B \cos q_1 - m_B l_A \rho_B \cos q_2 & m_D l_A l_C \cos q_1 - m_D l_A l_C \cos q_3 + m_E l_A l_C \cos q_1 - m_E l_A l_C \cos q_3 + m_C l_A \rho_C \cos q_1 - m_C l_A \rho_C \cos q_3 & m_E l_A l_D \cos q_1 - m_E l_A l_D \cos q_4 + m_D l_A \rho_D \cos q_1 - m_D l_A \rho_D \cos q_4 & m_E l_A \rho_E \cos q_1 - m_E l_A \rho_E \cos q_5 \\ m_C l_A l_B \cos q_1 - m_C l_A l_B \cos q_2 + m_D l_B l_A \cos q_1 - m_D l_A l_B \cos q_2 + m_E l_A l_B \cos q_1 - m_E l_A l_B \cos q_2 + m_B l_A \rho_B \cos q_1 - m_B l_A \rho_B \cos q_2 & I_B^2 m_C + I_B^2 m_D + I_B^2 m_E I_B + m_B \rho_B^2 & m_D l_B l_C \cos q_2 - m_D l_B l_C \cos q_3 + m_E l_B l_C \cos q_2 - m_E l_B l_C \cos q_3 + m_C l_B \rho_C \cos q_2 - m_C l_B \rho_C \cos q_3 & m_E l_B l_D \cos q_2 - m_E l_B l_D \cos q_4 + m_D l_B \rho_D \cos q_2 - m_D l_B \rho_D \cos q_4 & m_E l_B \rho_E \cos q_2 - m_E l_B \rho_E \cos q_5 \\ m_D l_A l_C \cos q_1 - m_D l_A l_C \cos q_3 + m_E l_A l_C \cos q_1 - m_E l_A l_C \cos q_3 + m_C l_A \rho_C \cos q_1 - m_C l_A \rho_C \cos q_3 & m_D l_B l_C \cos q_2 - m_D l_B l_C \cos q_3 + m_E l_B l_C \cos q_2 - m_E l_B l_C \cos q_3 + m_C l_B \rho_C \cos q_2 - m_C l_B \rho_C \cos q_3 & I_C^2 m_D + I_C^2 m_E I_C + m_C \rho_C^2 & m_E l_C l_D \cos q_3 - m_E l_C l_D \cos q_4 + m_D l_C \rho_D \cos q_3 - m_D l_C \rho_D \cos q_4 & m_E l_C \rho_E \cos q_3 - m_E l_C \rho_E \cos q_5 \\ m_E l_A l_D \cos q_1 - m_E l_A l_D \cos q_4 + m_D l_A \rho_D \cos q_1 - m_D l_A \rho_D \cos q_4 & m_E l_B l_D \cos q_2 - m_E l_B l_D \cos q_4 + m_D l_B \rho_D \cos q_2 - m_D l_B \rho_D \cos q_4 & m_E l_C l_D \cos q_3 - m_E l_C l_D \cos q_4 + m_D l_C \rho_D \cos q_3 - m_D l_C \rho_D \cos q_4 & I_D^2 m_E + I_D + m_D \rho_D^2 & m_E l_D \rho_E \cos q_4 - m_E l_D \rho_E \cos q_5 \\ m_E l_A \rho_E \cos q_1 - m_E l_A \rho_E \cos q_5 & m_E l_B \rho_E \cos q_2 - m_E l_B \rho_E \cos q_5 & m_E l_C \rho_E \cos q_3 - m_E l_C \rho_E \cos q_5 & m_E l_D \rho_E \cos q_4 - m_E l_D \rho_E \cos q_5 & I_E + m_E \rho_E^2 \end{bmatrix} \begin{bmatrix} \ddot{q}_1 \\ \ddot{q}_2 \\ \ddot{q}_3 \\ \ddot{q}_4 \\ \ddot{q}_5 \end{bmatrix} = \begin{bmatrix} (\tau_{N/A} - \tau_{A/B}) \cdot \hat{n}_3 \\ (\tau_{A/B} - \tau_{B/C}) \cdot \hat{n}_3 \\ (\tau_{B/C} - \tau_{C/D}) \cdot \hat{n}_3 \\ (\tau_{C/D} - \tau_{D/E}) \cdot \hat{n}_3 \\ (\tau_{D/E}) \cdot \hat{n}_3 \end{bmatrix} + \begin{bmatrix} f_2(l_A \cos q_1) - f_1(l_A \sin q_1) \\ f_2(l_B \cos q_2) - f_1(l_B \sin q_2) \\ f_2(l_C \cos q_3) - f_1(l_C \sin q_3) \\ f_2(l_D \cos q_4) - f_1(l_D \sin q_4) \\ f_2(l_E \cos q_5) - f_1(l_E \cos q_5) \end{bmatrix} + \begin{bmatrix} -\rho_A \cos q_1 & -l_A \cos q_1 & -l_A \cos q_1 & -l_A \cos q_1 & -l_A \cos q_1 \\ 0 & -\rho_B \cos q_2 & -l_B \cos q_2 & -l_B \cos q_2 & -l_B \cos q_2 \\ 0 & 0 & -\rho_C \cos q_3 & -l_C \cos q_3 & -l_C \cos q_3 \\ 0 & 0 & 0 & -\rho_D \cos q_4 & -l_D \cos q_4 \\ 0 & 0 & 0 & 0 & -\rho_E \cos q_5 \end{bmatrix} \begin{bmatrix} m_A g \\ m_B g \\ m_C g \\ m_D g \\ m_E g \end{bmatrix} \quad (55)$$

By rearranging the Eq. (54) and Eq. (55), the value of joint torque at each joint can be calculated.

3. Results

The goal of this study is to develop a three-dimensional dynamic model of the spine. The model evaluation provided evidence that the result obtained from mathematical model was reliable. All the calculations were carried out in MATLAB and Microsoft Excel.

3.1 Muscle Activities

The muscle activities were evaluated using the root mean square (RMS) to determine the activation level of back muscle during lifting. RMS value was chosen because it is one of the parameters that is most frequently used in scientific research and because it is more accurately depicts the levels of muscular activity both at rest and during contraction [26]. Also, RMS is important to point out the muscle activation strength [27]. Figure 5 indicates the average RMS values for each muscle involved. The bar graph illustrated the average RMS of the left and right erector spinae, latissimus dorsi, external oblique and internal oblique for all seven subjects. There is a clear difference in RMS of muscle activity. Muscle with the highest RMS value was internal oblique (IO) followed by external oblique (EO). Meanwhile, latissimus dorsi (LD) had the lowest RMS values where both right and left muscle were lowest in RMS when compared to other back muscles.

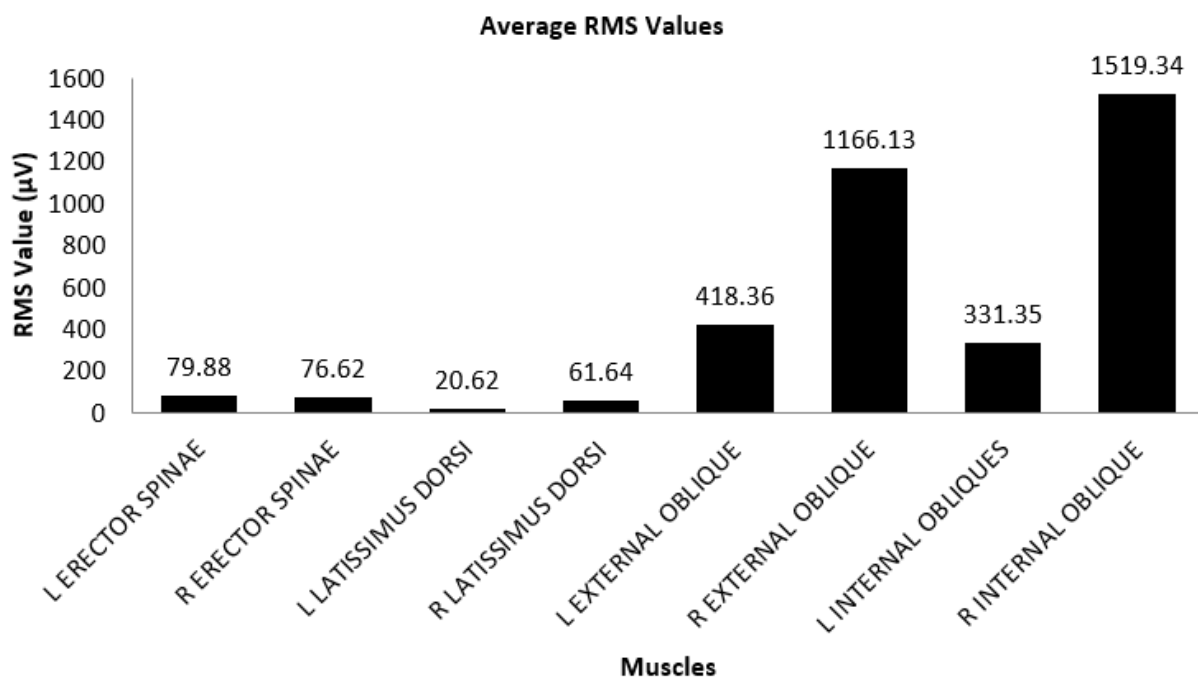


Fig. 5. Average root mean square (RMS) during lifting activity on different back muscles

The distributions of RMS are different between each muscle. Internal oblique muscle demonstrated the highest muscle activity followed by external oblique, erector spinae and latissimus dorsi. This can be explained as muscle activity tended to be redistributed to the lumbar region during lifting [28]. The subject also tend to perform right lateral bending during lifting movement which might impact a difference in right and left external and internal oblique. The beginning phase of trunk extension motion (pre-bending) is initiated by pelvis moment while the ending phase (post-bending) is achieved mainly by lumbar spine extension motion [29]. So, the EMG redistribution may be related to the duration of the lumbar muscles are active as depicted in [28,30].

3.2 Mathematical Model using Gordon's Method

Gordon's method was used to evaluate the value of torques during rotation at L5. Based on calculation result from Gordon's method, the developed mathematical model was able to give a good performance. Figure 6 illustrated the graph of average torques at L5 calculate from all subjects.

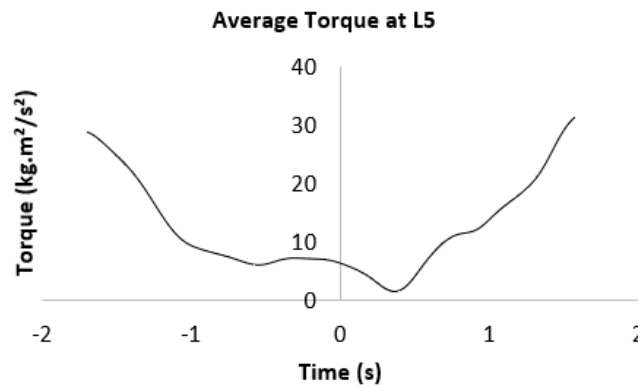


Fig. 6. Average torque at L5 of all subjects

In order to evaluate the mathematical model, this study compares the value of torque at L5 during bending with previous studies [31,32]. At time zero, subject was performing maximal bending. Torque estimates from the model at L5 during lifting activity agreed well with published values. Since this study is in consistent with the previous studies, the Gordon's method was extended to calculate torque at L3, L1, MAI and T2 during lifting activity. Figure 7 illustrated the torques at L3, L1, MAI and T2.

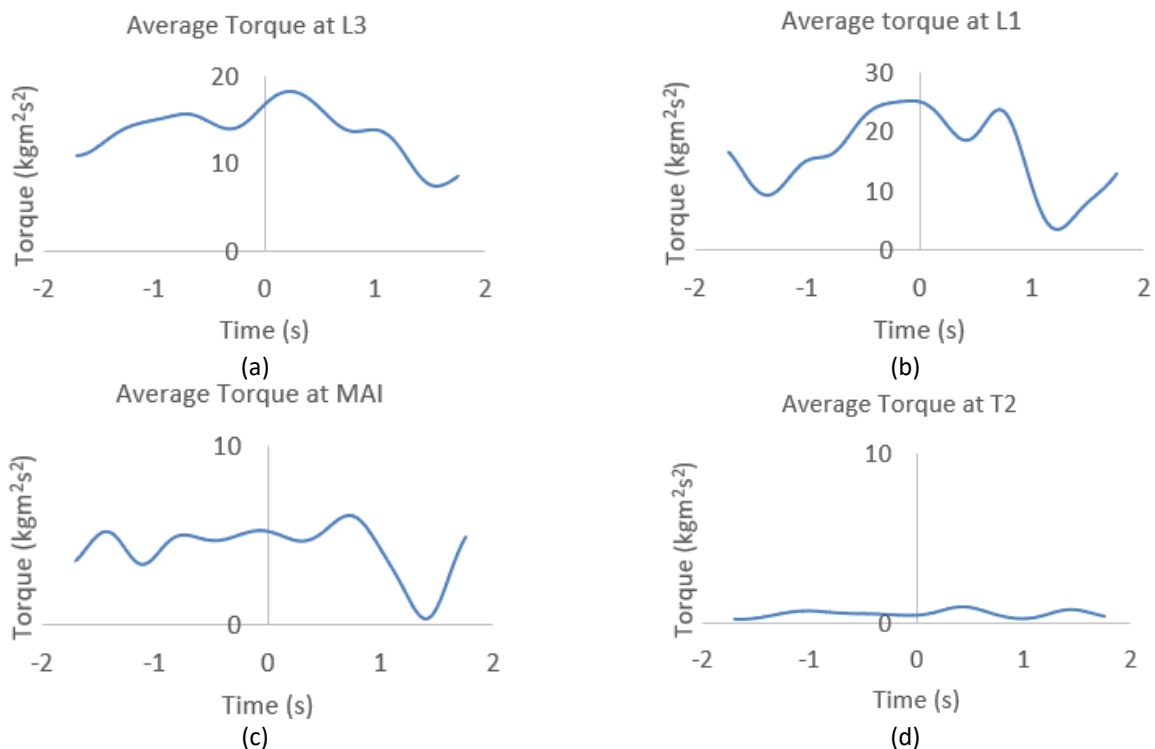


Fig. 7. Average torque at L3, L1, MAI and T2 during lifting activity for all subjects: a) average torque at L5 b) average torque at L1 c) average torque at MAI d) average torque at T2

Table 3 shows the average peak of torques during lifting activity where L1 produced greater torques during lifting activity followed by L3, MAI, L5 and T2. The validation of the torque at L5 served as a good example of the validation techniques employed for the entire model.

Table 3
 Mass, inertia and length estimates of vertebral segments

Joint	L5	L3	L1	MAI	T2
Average of Torque ($\text{kgm}^2\text{s}^{-2}$)	0 – 30	7 - 18	0 - 25	0 - 6	0 - 1

During lifting activity, the average torque value at L5 was $0 - 30 \text{ kgm}^2/\text{s}^2$, which indicated safe lifting load for healthy subject and less dangerous than the maximum permissible limit of $30-40 \text{ kgm}^2\text{s}^{-2}$ reported by Brosche *et al.*, [31] and Dolan & Adams [32]. Hence, the comparison shows a good agreement with the value obtained in this study where the values do not exceed the limit for healthy subject recommended by previous studies. The average torque value at L3, L1, MAI, and T2 were $7 - 18 \text{ kgm}^2\text{s}^{-2}$, $0 - 25 \text{ kgm}^2\text{s}^{-2}$, $0 - 6 \text{ kgm}^2\text{s}^{-2}$, $0 - 1 \text{ kgm}^2\text{s}^{-2}$, respectively. When looking at time zero (the time subjects performing maximal bending), the highest torque exerted were at L5, L3 and L1.

4. Conclusions

This study was conducted to develop a three-dimensional dynamic model for the spine during lifting activities comprises of five joints at L5, L3, L1, MAI and T2. The model was developed using Gordon method, which is a vector approach method for determining velocity and acceleration. The method introduces several important quantities for constructing dynamic equations of motion such as generalized velocity, partial linear velocity, partial angular velocity, generalised active force and generalised inertial force. Kinematic data obtained through experimental study was processed using Visual3D software by applying the Visual3D pipeline and computed using spline method as being done by previous study [33]. All the kinematic values were then used as an input in the mathematical model of the spine developed using Gordon's method. The model was initially evaluated before being used to estimate the joint torques during lifting.

The evaluation of the joint torque at L5 was compared to previous studies [31,32], and the result shows the model is adequate to estimate joint torque values at L3, L1, MAI and T2. Lifting demands a greater support from lumbar spine [34]. During maximal bending, the highest torque exerted were at L5, L3 and L1. This result is in agreement with EMG study where external oblique muscle and internal oblique located at lumbar body produced higher muscle activity during lifting. External oblique muscle generated large flexion moments during the extension during lifting [35]. Internal oblique acts to stabilize the spine and to compensate the fatigue of trunk muscles during repetitive trunk movements [36]. Hence, internal oblique increases their activity to compensate fatigue and the increase in muscle activation increase in spinal stability [36]. In fact, lumbar could be often damaged mechanically due to the asymmetric or unbalanced lifting movement where the heavy weight of an object is a critical factor to the lumbar damage [37]. The weakness on lumbar muscles been proposed to contribute to lumbar spine during lifting [38]. Decreased ability of the muscle to produce force may contribute to greater lumbar flexion during lifting [34].

5. Strength and Limitations

Gordon's method has been used to develop the mathematical model consists of 5 joints, namely L5, L3, L1, MAI and T2. The benefit of Gordon's method is that the equations of motion can be written in the most compact form as this method is constrained to open and unbranched kinematic chain. Therefore, Gordon's method can help in deriving the equations of motion of more complicated model; i.e., whole body model consists of all segments. The study used bimodal approach – EMG analysis and mathematical model. EMG analysis showed that high muscle activity can be seen at internal and external oblique muscles. These results support the estimation of value of torque using the mathematical model where L5, L3 and L1 shows higher joint torque values compared to the other three joint.

However, this study has limitations as the results may vary from one individual to another [21]. The variation might be because of the subject sometimes sweat during data collection and sweat build up beneath the electrodes may cause the EMG amplitude to become more sensitive [28]. There is also possibility that RMS is influenced by individual factors such as sensor location as stated in previous studies [27-29], body fat and individual skin condition [39]. As the task in this study conducted in repetitive condition, it is expected to accumulation of fatigued due to the subsequent changes of trunk motion and muscle activity [40]. Also, sample size remain is one of the limitations of this study. Only seven from ten subjects were analyzed as other three subjects were underrepresented in the data due to marker occlusion. Future work will incorporate the data of additional subjects to determine the significance of variables. However, analyzing more subjects may require many more hours of work, and the challenge in recruiting suitable subjects. Situations where retro-reflective markers continually fell off during the lifting were also an issue. After several trials of lifting, sweat began to accumulate on the skin of the subject and the markers to fall off more easily. So, before continuing the experiment, the markers need to be replaced, which might reduce the accuracy of the data.

Acknowledgement

This research was funded by a grant from Ministry of Higher Education of Malaysia (FRGS Grant FRGS/1/2018/STG06/UNIMAP/03/2).

References

- [1] Das, Sanjib Kumar, Vishal Singh Patyal, and Sudhir Ambekar. "Modeling of risk factors leading to workrelated musculoskeletal disorders in medical practitioners." *Safety Science* 172 (2024): 106427. <https://doi.org/10.1016/j.ssci.2024.106427>
- [2] Yang, Feng, Niu Di, Wei-wei Guo, Wen-bin Ding, Ning Jia, Hengdong Zhang, Dongxia Li et al. "The prevalence and risk factors of work related musculoskeletal disorders among electronics manufacturing workers: a cross-sectional analytical study in China." *BMC Public Health* 23, no. 1 (2023): 10. <https://doi.org/10.1186/s12889-022-14952-6>
- [3] Conforti, Ilaria, Ilaria Mileti, Zaccaria Del Prete, and Eduardo Palermo. "Measuring biomechanical risk in lifting load tasks through wearable system and machine-learning approach." *Sensors* 20, no. 6 (2020): 1557. <http://dx.doi.org/10.3390/s20061557>
- [4] Panjabi, Manohar M. "Three-dimensional mathematical model of the human spine structure." *Journal of Biomechanics* 6, no. 6 (1973): 671-680.
- [5] Panjabi, Manohar M., Richard A. Brand Jr, and Augustus A. White III. "Three-dimensional flexibility and stiffness properties of the human thoracic spine." *Journal of biomechanics* 9, no. 4 (1976): 185-192.
- [6] Bassani, Tito, Elena Stucovitz, Zhihui Qian, Matteo Briguglio, and Fabio Galbusera. "Validation of the AnyBody full body musculoskeletal model in computing lumbar spine loads at L4L5 level." *Journal of biomechanics* 58 (2017): 89-96. <http://dx.doi.org/10.1016/j.jbiomech.2017.04.025>

- [7] Actis, Jason A., Jasmin D. Honegger, Deanna H. Gates, Anthony J. Petrella, Luis A. Nolasco, and Anne K. Silverman. "Validation of lumbar spine loading from a musculoskeletal model including the lower limbs and lumbar spine." *Journal of Biomechanics* 68 (2018): 107-114. <https://doi.org/10.1016/j.jbiomech.2017.12.001>
- [8] Harari, Yaar, Avital Bechar, and Raziel Riemer. "Workers' biomechanical loads and kinematics during multiple-task manual material handling." *Applied ergonomics* 83 (2020): 102985. <https://doi.org/10.1016/j.apergo.2019.102985>
- [9] Selamat, Hazlina, Tahmida Islam, Mohamad Fadzli Haniff, and Ahmad Jais Alimin. "Design and Implementation of Hybrid Exoskeleton for Oil Palm Harvester to Reduce Muscle Strain." *Journal of Advanced Research in Applied Mechanics* 105, no. 1 (2023): 1-11. <https://doi.org/10.37934/aram.105.1.111>
- [10] Yamaguchi, Gary Tad, and Gary Tad Yamaguchi. "Chapter 6 Dynamic Equations of Motion." *Dynamic Modeling of Musculoskeletal Motion: A Vectorized Approach for Biomechanical Analysis in Three Dimensions* (2001): 173-206.
- [11] Zulkifli, Wan Nur Syazana Wan, Wan Rozita Wan Din, and Azmin Sham. "Modeling of Shooter Position Using Gordon's Method." *Global Journal of Pure and Applied Mathematics* 11, no. 2 (2015): 625-633.
- [12] Leardini, Alberto, Fabio Biagi, Andrea Merlo, Claudio Belvedere, and Maria Grazia Benedetti. "Multi-segment trunk kinematics during locomotion and elementary exercises." *Clinical Biomechanics* 26, no. 6 (2011): 562-571. [10.1016/j.clinbiomech.2011.01.015](https://doi.org/10.1016/j.clinbiomech.2011.01.015)
- [13] Han, Kap-Soo, Thomas Zander, William R. Taylor, and Antonius Rohlmann. "An enhanced and validated generic thoraco-lumbar spine model for prediction of muscle forces." *Medical engineering & physics* 34, no. 6 (2012): 709-716. <http://dx.doi.org/10.1016/j.medengphy.2011.09.014>
- [14] Arshad, Rizwan, Thomas Zander, Maxim Bashkuev, and Hendrik Schmidt. "Influence of spinal disc translational stiffness on the lumbar spinal loads, ligament forces and trunk muscle forces during upper body inclination." *Medical Engineering & Physics* 46 (2017): 54-62. <http://dx.doi.org/10.1016/j.medengphy.2017.05.006>
- [15] Weston, Eric B., Jonathan S. Dufour, Ming-Lun Lu, and William S. Marras. "Spinal loading and lift style in confined vertical space." *Applied Ergonomics* 84 (2020): 103021. <https://doi.org/10.1016/j.apergo.2019.103021>
- [16] Subramaniyam, Murali, Seung Nam Min, Se Jin Park, and Sangho Park. "Muscle activity and spinal loading in lifting symmetrical loads beside the body compared to in front of the body." *Journal of Mechanical Science and Technology* 29 (2015): 5075-5081. <http://dx.doi.org/10.1007/s12206-015-1104-z>
- [17] Granata, Kevin P., and W. S. Marras. "An EMG-assisted model of trunk loading during free-dynamic lifting." *Journal of biomechanics* 28, no. 11 (1995): 1309-1317.
- [18] Kogami, Tonan, Ai Higuchi, and Tomohiro Shibata. "Fatigue assessment using surface emg on lifting motions." In *2022 IEEE 4th Global Conference on Life Sciences and Technologies (LifeTech)*, pp. 425-426. IEEE, 2022. <http://dx.doi.org/10.1109/LifeTech53646.2022.9754833>
- [19] Yong, Xu, Zefeng Yan, Can Wang, Chao Wang, Nan Li, and Xinyu Wu. "Ergonomic mechanical design and assessment of a waist assist exoskeleton for reducing lumbar loads during lifting task." *Micromachines* 10, no. 7 (2019): 463. <http://dx.doi.org/10.3390/mi10070463>
- [20] Pranata, Adrian, Luke Perraton, Doa El-Ansary, Ross Clark, Benjamin Mentiplay, Karine Fortin, B. Long, Robert Brandham, and A. L. Bryant. "Trunk and lower limb coordination during lifting in people with and without chronic low back pain." *Journal of biomechanics* 71 (2018): 257-263. <https://doi.org/10.1016/j.jbiomech.2018.02.016>
- [21] Jelti, Z., Kevin Lebel, B. Letellier, and Pierre RL Slangen. "Motion capture and myoelectric multimodal measurements during static and dynamic bending tasks using a back-assisting exoskeleton: a preliminary study." In *Multimodal Sensing and Artificial Intelligence: Technologies and Applications II*, vol. 11785, pp. 90-103. SPIE, 2021. <http://dx.doi.org/10.1117/12.2593283>
- [22] Totah, Deema, Lauro Ojeda, Daniel D. Johnson, Deanna Gates, Emily Mower Provost, and Kira Barton. "Low-back electromyography (EMG) data-driven load classification for dynamic lifting tasks." *PloS one* 13, no. 2 (2018): e0192938. <https://doi.org/10.1371/journal.pone.0192938>
- [23] Nur, Nurhayati Mohd, Siti Zawiah Md Dawal, Mahidzal Dahari, and Junedah Sanusi. "Muscle activity, time to fatigue, and maximum task duration at different levels of production standard time." *Journal of physical therapy science* 27, no. 7 (2015): 2323-2326. <https://doi.org/10.1589/jpts.27.2323>
- [24] Singh, Jaskaran, Kavita Pahuja, and Dr JK Geeta. "Correlation of body height with thoracic and lumbar vertebral parameters." *Indian Journal of Basic and Applied Medical Research* 4, no. 1 (2014): 144-153.
- [25] Pearsall, David J., J. Gavin Reid, and Lori A. Livingston. "Segmental inertial parameters of the human trunk as determined from computed tomography." *Annals of biomedical engineering* 24 (1996): 198-210. <https://doi.org/10.1007/BF02667349>
- [26] Fukuda, Thiago Yukio, Jorge Oliveira Echeimberg, José Eduardo Pompeu, Paulo Roberto Garcia Lucareli, Silvio Garbelotti, Rafaela Okano Gimenes, and Adilson Apolinário. "Root mean square value of the electromyographic signal in the isometric torque of the quadriceps, hamstrings and brachial biceps muscles in female subjects." *J Appl Res* 10, no. 1 (2010): 32-39.

- [27] Salleh, Noor Azlina Mohd, Muhammad Syukran Al-Baria Noor Sazali, Noor Ayuni Che Zakaria, Nadia Mohd Mustafah, and Aizreena Azaman. "Electromyography Analysis of Lower Extremity Muscles during Squat and Stoop Movement." In *IOP Conference Series: Materials Science and Engineering*, vol. 834, no. 1, p. 012035. IOP Publishing, 2020. <http://dx.doi.org/10.1088/1757-899X/834/1/012035>
- [28] Dos Anjos, F. V., M. Ghislieri, G. L. Cerone, T. P. Pinto, and M. Gazzoni. "Changes in the distribution of muscle activity when using a passive trunk exoskeleton depend on the type of working task: A high-density surface EMG study." *Journal of Biomechanics* 130 (2022): 110846. <https://doi.org/10.1016/j.jbiomech.2021.110846>
- [29] Hu, Boyi, and Xiaopeng Ning. "The changes of trunk motion rhythm and spinal loading during trunk flexion and extension motions caused by lumbar muscle fatigue." *Annals of biomedical engineering* 43 (2015): 2112-2119. <http://dx.doi.org/10.1007/s10439-015-1248-0>
- [30] Błaszczuk, Anna, and Małgorzata B. Ogurkowska. "The use of electromyography and kinematic measurements of the lumbar spine during ergonomic intervention among workers of the production line of a foundry." *PeerJ* 10 (2022): e13072. <http://dx.doi.org/10.7717/peerj.13072>
- [31] Brosche, Justus, Hannes Wackerle, Peter Augat, and Hermann Lödding. "A Learning Assistance System for the Ergonomic Behavioural Prevention in Production." *Competence development and learning assistance systems for the data-driven future: GITO* (2021): 93-108. https://doi.org/10.30844/wgab_2021_6
- [32] Dolan, P., and M. A. Adams. "Influence of lumbar and hip mobility on the bending stresses acting on the lumbar spine." *Clinical Biomechanics* 8, no. 4 (1993): 185-192. [https://doi.org/10.1016/0268-0033\(93\)90013-8](https://doi.org/10.1016/0268-0033(93)90013-8)
- [33] Omar, Nurhidayah. "Technique in overarm throwing." PhD diss., Loughborough University, 2016.
- [34] Patterson, Christopher S., Everett Lohman, Skulpan Asavasopon, Robert Dudley, Lida Gharibvand, and Christopher M. Powers. "The influence of hip flexion mobility and lumbar spine extensor strength on lumbar spine flexion during a squat lift." *Musculoskeletal Science and Practice* 58 (2022): 102501. <https://doi.org/10.1016/j.msksp.2021.102501>
- [35] Granata, Kevin P., and W. S. Marras. "The influence of trunk muscle coactivity on dynamic spinal loads." *Spine* 20, no. 8 (1995): 913-919.
- [36] Larivière, Christian, Denis Gagnon, and Patrick Loisel. "The comparison of trunk muscles EMG activation between subjects with and without chronic low back pain during flexion–extension and lateral bending tasks." *Journal of electromyography and kinesiology* 10, no. 2 (2000): 79-91. [https://doi.org/10.1016/S1050-6411\(99\)00027-9](https://doi.org/10.1016/S1050-6411(99)00027-9)
- [37] Hwang, Seonhong, Youngeun Kim, and Youngho Kim. "Lower extremity joint kinetics and lumbar curvature during squat and stoop lifting." *BMC musculoskeletal disorders* 10 (2009): 1-10. <https://doi.org/10.1186/1471-2474-10-15>
- [38] Zhu, Rui, Wen-xin Niu, Zhi-li Zeng, Jian-hua Tong, Zhi-wei Zhen, Shuang Zhou, Yan Yu, and Li-ming Cheng. "The effects of muscle weakness on degenerative spondylolisthesis: A finite element study." *Clinical Biomechanics* 41 (2017): 34-38. <https://doi.org/10.1016/j.clinbiomech.2016.11.007>
- [39] Kleine, B-U., N-P. Schumann, I. Bradl, R. Grieshaber, and H-C. Scholle. "Surface EMG of shoulder and back muscles and posture analysis in secretaries typing at visual display units." *International archives of occupational and environmental health* 72 (1999): 387-394. <https://doi.org/10.1007/s004200050390>
- [40] Davis, Kermit G., and William S. Marras. "Assessment of the relationship between box weight and trunk kinematics: does a reduction in box weight necessarily correspond to a decrease in spinal loading?." *Human factors* 42, no. 2 (2000): 195-208. <https://doi.org/10.1518/001872000779656499>